Simulation of a Moving Bed Gasifier for a Western Coal

This paper describes an adiabatic steady state plug flow model for a moving bed coal gasifier with gas-solid heat transfer. The model considers 17 solid stream components, 10 gas stream components and 17 reactions. The kinetic and thermodynamic parameters were derived for a Wyoming subbituminous coal. Examples of calculated results are given.

Introduction

A moving bed gasifier is a vertical countercurrent reactor in which the solids stream moves slowly downward through the reactor while the gas stream flows upward. Coal is added at the top of the reactor and ash (and/or clinker or molten slag) is removed from the bottom. The term fixed bed is sometimes used to describe this reactor since normally the top of the coal bed is maintained at a fairly constant level. A mixture of steam and oxygen (or air) is fed to the bottom of the reactor to provide some of the reactants for the combustion and gasification of the coal.

The plug flow version (no backmixing) of the gasifier is described here. The mass and energy balances will be given along with the kinetic, equilibrium, and thermodynamic equations used for the steady state simulation model.

Reaction events

To form a basis for the development of a simulation model, it is convenient to postulate a sequence of physical and chemical events in the gasifier. The following series of events is assumed to take place in the reactor as the solids stream flows downward against the rising gas stream.

● Event 1. Drying

The temperature of the moist coal is increased and the coal moisture is evaporated by heat exchange between the coal and the hot gas stream.

• Event 2. Devolatilization

The temperature of the dry coal is increased further and volatile products are released from the coal, leaving a char.

• Event 3. Gasification

Some of the char is gasified by reacting with the H_2 , CO_2 , and H_2O components in the gas stream.

• Event 4. Combustion

The remaining char is burned, using oxygen in the feed gas and leaving an ash residue. Depending upon the conditions in the reactor, some or all of the ash may melt and then either solidify to form clinkers or else remain in a molten state (slag).

Reaction components

The number of chemical components which occur within the reactor is very large. Many of these components occur in very small amounts or do not have an appreciable effect on the operation of the reactor. As a first approach to the reactor simulation, a set of components was selected which contains most of the components thought to be important and yet is of a relatively small size. The following 17 components are considered in the solids stream:

 H_2O , H_2 , N_2 , O_2 , C, S, ash, slag, clinker, $H_2O(vs)$, $H_2(vs)$, $CO_2(vs)$, CO(vs), $CH_4(vs)$, $H_2S(vs)$, $NH_3(vs)$, tar(vs),

where (vs) indicates volatile solids.

Copyright 1979 by International Business Machines Corporation. Copyring is permitted without payment of royalty provided that (1) each reproduction is done without alteration and (2) the *Journal* reference and IBM copyright notice are included on the first page. The title and abstract may be used without further permission in computer-based and other information-service systems. Permission to *republish* other excerpts should be obtained from the Editor.

For the gas stream, the following 10 components are considered:

At a future date, additional components may be considered for the gas and solids streams. Possible candidates include

Reaction equations

A set of coal gasification reactions can now be written for the preceding events.

• Event 1. Drying

Moist coal
$$\rightarrow$$
 Dry coal + H_oO (1)

• Event 2. Devolatilization

Dry coal
$$\rightarrow$$
 Char + Volatiles (2)-(9)

• Event 3. Gasification

$$Char + H_{o}O \rightarrow CO + H_{o}$$
 (10)

$$Char + CO_{g} \rightarrow 2CO \tag{11}$$

$$Char + 2H_2 \rightarrow CH_4 \tag{12}$$

$$CO + H_{o}O \rightleftharpoons CO_{o} + H_{o}$$
 (13)

$$CO + 3H_{3} \rightleftharpoons CH_{4} + H_{3}O \tag{14}$$

It is also possible for the following carbon deposition reactions to occur:

$$CO + H_o \rightleftharpoons C + H_o O$$
 (10a)

$$2CO \rightleftharpoons C + CO_a$$
 (11a)

$$CH_4 \rightleftharpoons C + 2H_2$$
 (12a)

However, (10a), (11a), and (12a) will not be considered at this time. The dissociation reactions of CO, CO_2 , H_2O , H_2 , and O_2 also will not be considered at this time.

• Event 4. Combustion

$$\zeta \text{Char} + O_2 \rightarrow \text{Ash} + 2(\zeta - 1)\text{CO} + (2 - \zeta)\text{CO}_2$$
 (15)

$$Ash \rightarrow Slag$$
 (16)

$$Slag \rightarrow Clinker$$
 (17)

The value of the stoichiometric constant ζ determines the distribution of CO and CO₂ in the primary combustion products and is in the range of 1 to 2.

Kinetic equations

The set of rate equations which are used for the reactions listed above are as follows.

• Event 1. Drying

The three drying models (exponential rate, receding wet core-dry shell, and constant rate) discussed by McIntosh [1, 2] were considered for this event. He found that the simple constant rate model predicted drying conditions about as well as the more complicated models. Therefore, the convection drying of the coal is handled by using a base drying rate value for surface water evaporation followed by a falling rate value when the water concentration falls below the critical moisture content. The base rate value is given by

$$(rate)_1 = R_c = C_1/[1.0 + \exp(A_1 - B_1T_S)],$$

where $R_{\rm c}$ is the base drying rate in moles of water evaporated per minute per unit volume of reactor. $A_{\rm l}$, $B_{\rm l}$, and $C_{\rm l}$ are constants and $T_{\rm s}$ is the absolute temperature of the solids. The falling rate value is given by

$$(rate)_1 = R_c X_w / X_c$$

where it has been assumed that the equilibrium moisture content of the coal is zero at the conditions existing in the gasifier. The critical moisture content of the coal X_c is expressed in mole fraction and X_w is the moisture mole fraction in the solids and is in the range

$$0 \le X_{\rm w} \le X_{\rm c}$$
.

• Event 2. Devolatilization

Most of the pyrolysis data have been obtained from rapid or very fast heating rate experiments and are of little use for fixed bed gasifiers since the distribution of volatile products from this reaction depends on the heating rate and the coal type. Campbell [3–5] conducted pyrolysis experiments with Wyoming subbituminous coal at a heating rate of 0.0555° C/s. Since this is closer to the heating rates found in fixed bed gasifiers (≈ 0.1 to 5° C/s) than are the rates in rapid to very fast heating rate experiments ($\approx 10^3$ to 10^5 °C/s), his data were used to develop the kinetic equations for this event.

The yield and distribution of the individual volatile products released from the coal are calculated using a set of 8 independent parallel first-order equations,

$$(rate)_i = k_i C_i$$
 $i = 2, 3, \dots, 9,$

where the 8 constituents are the CO_2 , CO, H_2 , CH_4 , H_2O , NH_3 , H_2S , and tar in the volatile solids. The rate of reaction has the units of moles of volatile component j per minute per unit volume of reactor. C_j is the concentration of volatile component j in moles per unit volume of reactor and k_j is the first-order rate constant for reaction i in reciprocal minutes. The rate constant is assumed to have the standard Arrhenius form

$$k_i = A_i \exp(-E_i/R_G T_S)$$
 $i = 2, 3, \dots, 9,$

241

where A_i is the frequency factor for reaction i in reciprocal minutes, E_i is the activation energy for reaction i in energy per mole, $R_{\rm G}$ is the gas constant in energy per mole per absolute degree, and $T_{\rm S}$ is the absolute temperature of the solids.

• Event 3. Gasification

The model proposed by Dutta et al. [6] was used as a guide to develop the gasification kinetic model used in this work. Their kinetic model includes a factor for change in available pore surface area during the course of a reaction, and a modified form of an effectiveness factor that accounts for diffusional resistance within the solid particle at higher reaction temperatures.

The data given by Taylor and Bowen [7], Gibson and Euker [8], and Fischer *et al*. [9] were used to develop the kinetic parameters for the char-steam reaction. The charcarbon dioxide reaction parameters were developed from data given by Taylor and Bowen [7] and Hippo and Walker [10]. The kinetic parameters for the char-hydrogen reaction were derived by using the hydrogasification data of Pyrcioch *et al*. [11] and the reactivity data of Tomita, Mahajan, and Walker [12].

Equations (10), (11), and (12) for this event represent irreversible heterogeneous gas-solid reactions. The following rate equations are used for these reactions:

$$(rate)_i = \eta_i a \ k_i C_e C_{iG}$$
 $i = 10, 11, 12,$

where the rate of reaction is expressed in moles of carbon per minute per unit volume of reactor. C_c is the concentration of the carbon in the solids in moles per unit volume of reactor, C_{jG} is the concentration of component j in the gas stream in moles per unit volume, and a is the effective surface area ratio of the char. The j components for these reactions are H_2O , CO_2 , and H_2 , respectively.

The rate constant has the Arrhenius form

$$k_i = A_i \exp(-E_i/R_cT_s)$$
 $i = 10, 11, 12,$

where k_i now is in volume per minute per mole of component j.

The effective surface area ratio of the char for these reactions is given by

$$a = 2 + 100X^{c_1} \exp(-c_2X) - \exp(c_2X),$$

where X is the fractional conversion of the carbon and c_1 , c_2 , and c_3 are constants; c_1 is in the range of 1 to 2.

The equation used for the effectiveness factor is

$$\eta_i = 3 \{ [1/\tanh(M_i) - 1/M_i] \} / M_i \quad i = 10, 11, 12,$$

where the modified Thiele modulus is

$$M_i = \phi_i \sqrt{a(1-X)}$$
 $i = 10, 11, 12.$

The initial Thiele modulus is defined by

$$\phi_i = R_p \sqrt{k_i (C_c)_{\text{initial}} / D_{ei}}$$
 $i = 10, 11, 12,$

where $R_{\rm p}$ is the solids particle radius, $(C_{\rm c})_{\rm initial}$ is the initial value for $C_{\rm c}$, and $D_{\rm ei}$ is the effective diffusivity of component j for reaction i in area per minute. This latter value is given by

$$D_{ei} = D_i (T_S)^{c_4} / P$$
 $i = 10, 11, 12;$

 c_4 is in the range of 1 to 2. The D_i and c_4 are constants and P is the absolute pressure in the reactor.

Most of the water-gas shift reaction equations presented in the literature were not thermodynamically consistent and hence are not very useful for calculations in the vicinity of equilibrium.

The second-order data presented by Moe [13] are thermodynamically consistent and were used to develop the kinetic parameters for the shift reaction. It should be noted that his data are based on space velocity time and must be adjusted for real time before being used. Wen [14] also gives a kinetic equation that is similar to the one given by Moe.

As with the shift reaction, most of the methanation results presented in the literature represent empirical fits to data and are not thermodynamically consistent. Vatcha [15] took the rate expression developed at the Institute of Gas Technology (Chicago) by Lee [16] and modified it to a thermodynamically consistent Langmuir-Hinshelwood form. A power law version of the Vatcha equation was used to simulate this reaction in our model.

The shift and methanation reactions, (13) and (14) for Event 3, will be treated as reversible homogeneous gas phase reactions, with the mineral content of the ash acting as the catalyst for the reactions. The rate equations will then be

$$(rate)_{13} = \beta_{13} k_{13} (C_{C0} C_{H_2O} - C_{CO_2} C_{H_2} / K_{13}) C_{ash}$$

and

$$(rate)_{14} = \beta_{14} k_{14} (C_{\rm CO} C_{\rm H_2}^3 - C_{\rm CH_4} C_{\rm H_2O} / K_{14}) C_{\rm ash},$$

where the rates are expressed as moles of CO per minute per unit volume of reactor. $C_{\rm ash}$ is the concentration of ash in the solids in moles per unit volume of reactor. The remaining C are the appropriate gas stream concentrations in moles per unit volume, and the β represent the ratios of ash activity relative to commercial catalyst activ-

ity in weight of catalyst per mole of ash. The β are given as linear functions of carbon conversion:

$$\beta_i = \alpha_i + \alpha'_i X$$
 $i = 13, 14.$

The rate constants have the Arrhenius form

$$k_i = A_i \exp(-E_i/R_G T_G)$$
 $i = 13, 14,$

where $T_{\rm G}$ is the gas stream absolute temperature. The k_{13} value has the units of length to the sixth power per minute per mole ${\rm H_2O}$ per unit weight of catalyst, and k_{14} has the units of length to the twelfth power per minute per cubic mole ${\rm H_2}$ per unit weight of catalyst.

The K are the reaction equilibrium constants defined by

$$K_{13} = (C_{CO_2}C_{H_2}/C_{CO}C_{H_2O})_{\text{equilibrium}}$$
,

$$K_{14} = (C_{\text{CH}}C_{\text{HoO}}/C_{\text{CO}}C_{\text{Ho}}^3)_{\text{equilibrium}}$$

and they are calculated by

$$K_{13} = \exp \{ [(a_1/T_G) - a_2 \ln (T_G) + a_3 T_G - a_4 (T_G)^2 + a_5 (T_C)^3 + a_6] / R_C \},$$

$$K_{14} = \exp \{ [(b_1/T_G) - (b_2 - 2) \ln (T_G) + b_3 T_G + b_4 (T_G)^2 - b_5 (T_G)^3 + b_6] / R_G \}.$$

The K_{13} value is dimensionless, while K_{14} has the units of length to the sixth power per square mole. The constants needed for the above equilibrium equations were obtained from Shah and Stillman [17].

• Event 4. Combustion

The overall average equation for a shrinking-core model given by Levenspiel [18] was used as a guide to develop the kinetic model for combustion. The data contained in References [6a, 19-33] were specifically used to develop the kinetic parameters for the char-oxygen reaction. An Arrhenius plot of the data fell into two distinct bands, a carbon band and a coal/char band. This information was used to establish an estimate of the activation energy for the reaction. The reactivity data for Wyoming subbituminous coal in Jenkins, Nandi, and Walker [20] were then used to obtain the value of the frequency factor.

The ζ function in reaction (15), which gives the distribution of CO and CO₂ in the combustion products, will be calculated from the equation

$$\zeta = 2(R_{c} + 1)/(R_{c} + 2),$$

where R_x has the standard Arrhenius form

$$R_{z} = A_{z} \exp(-E_{z}/R_{G}T_{S}).$$

The kinetic constants for this equation were obtained from Arthur [34]. As can be seen, ζ approaches 1 for small R_{ζ} values and approaches 2 for large R_{ζ} values.

The combustion event itself will be considered to be an irreversible heterogeneous gas-solid reaction. The rate of combustion will be calculated by the first-order equation

$$(rate)_{15} = \bar{k}_{15} C_{0a}$$

where \bar{k}_{15} is the overall first-order rate constant in reciprocal minutes and C_{0_2} is the concentration of the oxygen in the gas stream in moles per unit volume. The reaction rate has the units of moles of oxygen per minute per unit volume of reactor.

The overall rate constant can be obtained from the relationship

$$\frac{1}{\bar{k}_{15}} = \frac{d_{\rm p}}{6k_{\rm f}} + \frac{d_{\rm p}^2}{24D_{\rm ea}} + \frac{3}{k_{\rm c}} ,$$

where $d_{\rm p}$ is the solids particle diameter for the combustion reaction, $k_{\rm f}$ is the film mass transfer coefficient in length per minute, $D_{\rm ea}$ is the effective rate of diffusion of the oxygen through the ash in area per minute (unreacted shrinking-core model), and $k_{\rm c}$ is the first-order reaction rate for the chemical reaction in reciprocal minutes.

The film coefficient is calculated from the equation

$$k_{\rm f} = D_{\rm f}(T_{\rm F})^{\rm cr}(1-\varepsilon)/\varepsilon P d_{\rm p},$$

where $D_{\rm f}$ and $c_{\rm f}$ are constants and $c_{\rm f}$ is in the range of 1 to 2, ε is the void fraction of the reactor bed, P is the absolute reactor pressure, and $T_{\rm F}$ is the absolute temperature, defined by

$$T_{\rm E} = (T_{\rm S} + T_{\rm G})/2.$$

The effective diffusivity of the oxygen through the ash is given by

$$D_{\rm ea} = D_{\rm a} (T_{\rm E})^{c_{\rm a}}/P,$$

where $D_{\rm a}$ and $c_{\rm a}$ are constants and $c_{\rm a}$ is in the range of 1 to 2. The first-order reaction rate for the chemical reaction between carbon and oxygen can be expressed as

$$k_e = \eta_{15} a k_{15} C_e / \zeta$$
,

where $C_{\rm c}$ is the concentration of the carbon in the solids in moles per unit volume of reactor and ζ is in moles of carbon reacted per mole of oxygen.

The rate constant has the Arrhenius form

$$k_{15} = A_{15} \exp(-E_{15}/R_{\rm G}T_{\rm S}),$$

where k_{15} has the units of volume per minute per mole of oxygen.

The effective surface area ratio of the char for combustion is given by

$$a = 2 + 100X^{c_1} \exp(-c_2X) - \exp(c_3X),$$

where X is the fractional conversion of the carbon and c_1 , c_2 , and c_3 are constants.

The effectiveness factor equation is

$$\eta_{15} = 3 \{ [1/\tanh(M_{15})] - 1/M_{15} \} / M_{15},$$

where the modified Thiele modulus is

$$M_{15} = \phi_{15} \sqrt{a(1-X)}$$

and the initial Thiele modulus is defined by

$$\phi_{15} = \frac{d_{\rm p}}{2} \sqrt{k_{15}(C_{\rm c})_{\rm initial}/D_{\rm e15}}$$
,

where $(C_e)_{\rm initial}$ is the initial value for C_e and $D_{\rm e15}$ is the effective diffusivity of oxygen through the char in area per minute. This value is given by

$$D_{e15} = D_{15}(T_{\rm S})^{c_4}/P$$

where D_{15} and c_4 are constants.

Simple heat-transfer-limited relationships were used for the ash melting and clinker forming reactions:

$$(rate)_{16} = C_{ash}C_{16}/[1 + \exp(A_{16} - B_{16}T_S)],$$

$$(rate)_{17} = C_{\text{slag}}C_{17}/[1 + \exp(B_{17}T_S - A_{17})],$$

where the reaction rates are expressed in moles per minute per unit volume of reactor; $C_{\rm ash}$ is the concentration of the ash in the solids in moles (MW = 67.39) per unit volume of reactor and $C_{\rm slag}$ is the concentration of slag in moles (MW = 67.39) per unit volume of reactor. A_{16} , B_{16} , C_{16} , A_{17} , B_{17} , and C_{17} are constants.

Steady state equations

The differential equation model for the steady state simulation of a moving bed coal gasifier will be derived directly from the continuity equations for mass and energy. In the model presented here, axial mass and energy dispersion will not be considered, and the reactor will be assumed to be operating adiabatically, so there will be no radial gradients for mass and energy.

The steady state mass balance equations for the solids stream are given by

$$\frac{d(F_{jS})}{dz} = \sum_{i} a_{ij} r_{i} \qquad i = 1, 2, \dots, 17, j = 1, 2, \dots, 17,$$

where F_{js} is the molar flux of component j in the solids in moles per minute per unit cross-sectional area of reactor, and is defined as

$$F_{ss} \equiv C_{ss}u_{s}$$
 $j = 1, 2, \cdots, 17.$

The concentration of solids component j, C_{jS} , is given in moles per unit volume of reactor, and u_{S} is the local velocity of the solids stream in length per minute.

The a_{ij} values represent the stoichiometric coefficients for component j in reaction i, r_i is the rate of the ith reaction in moles per minute per unit volume of reactor, and z is the distance from the bottom of the reactor.

The corresponding mass balance equations for the gas stream are given by

$$-\frac{d(F_{jG})}{dz} = \sum_{i} a_{ij} r_{i} \qquad i = 1, 2, \dots, 17, j = 18, 19, \dots, 27,$$

where $F_{j\rm G}$ is the molar flux of component j in the gas in moles per minute per unit cross-sectional area of reactor, and is defined as

$$F_{iG} \equiv C_{iG}u_{G}$$
 $j = 18, 19, \cdots, 27.$

The concentration of gas component j, $C_{j\rm G}$, is given in moles per unit volume of reactor, and $u_{\rm G}$ is the local gas velocity in length per minute. The minus sign for the gas flux indicates the countercurrent flow of gas and solids.

The steady state energy balance equation for the solids stream is

$$\frac{d(\psi_{S})}{dz} = h_{GS}A_{GS}(T_{G} - T_{S}) - \sum_{i} r_{i}\Delta H_{i}$$

$$i = 1, 2, \dots, 12, 15, 16, 17,$$

where $\psi_{\rm S}$ is the energy flux for the solids in energy per minute per unit cross-sectional area of reactor, and is defined as

$$\psi_{\rm c} \equiv c_{\rm pc} C_{\rm c} u_{\rm c} T_{\rm c}$$

where $C_{\rm S}$ is the total concentration of the solids in moles per unit volume of reactor. $T_{\rm S}$ is the solids temperature in absolute degrees and $c_{\rm pS}$ is the molar heat capacity of the solids in energy per mole per absolute degree, given by

$$c_{pS} = \sum_{j} x_{j} c_{pSj}$$
 $j = 1, 2, \dots, 17.$

The x_j are the mole fractions for the solid components, and the individual molar heat capacities in the solids are calculated from cubic polynomials:

$$c_{pSj} = a_{0Sj} + a_{1Sj}T_S + a_{2Sj}T_S^2 + a_{3Sj}T_S^3$$

 $j = 1, 2, \dots, 17.$

The first term on the right-hand side of the solids energy balance equation represents the heat being exchanged between the gas and the solids, and the last term is the gain and loss in heat resulting from the various reactions taking place in the solids. An exothermic reaction has a negative heat of reaction and an endothermic reaction has a positive heat of reaction. The local gas-solids heat transfer coefficient, $h_{\rm GS}$, is given in energy per minute per area per absolute degree. $A_{\rm GS}$ is the local gas-solids heat

transfer area in area per unit volume, $T_{\rm G}$ is the gas stream temperature in absolute degrees, and the ΔH_i are heats of reaction for the solids reactions in energy per mole. These latter values are calculated from quartic polynomials:

$$\Delta H_i = H_{ci} + b_{1i}T_G + b_{2i}T_G^2 + b_{3i}T_G^3 + b_{4i}T_G^4 + c_{1i}T_S$$
$$+ c_{2i}T_S^2 + c_{3i}T_S^3 + c_{4i}T_S^4 \qquad i = 1, 2, \dots, 17.$$

Of the 17 reactions considered here, 8 are endothermic, 8 are exothermic, and 1 changes from endothermic to exothermic as the temperature increases.

The corresponding steady state energy balance for the gas stream is

$$-\frac{d(\psi_{\rm G})}{dz} = -h_{\rm GS}A_{\rm GS}(T_{\rm G} - T_{\rm S}) - \sum_{i} r_{i}\Delta H_{i} \qquad i = 13, 14,$$

where ψ_G is the gas stream energy flux in energy per minute per unit cross-sectional area of reactor, and is defined as

$$\psi_{\rm G} \equiv c_{\rm pG} C_{\rm G} u_{\rm G} T_{\rm G}$$

The total concentration of the gas, $C_{\rm G}$, is given in moles per unit volume of reactor and $c_{\rm pG}$ is the gas molar heat capacity in energy per mole per absolute degree, given by

$$c_{pG} = \sum_{j} y_{j} c_{pGj}$$
 $j = 18, 19, \dots, 27.$

The y_j are the gas component mole fractions, and the individual gas molar heat capacities are calculated from cubic polynomials:

$$c_{pGj} = a_{0Gj} + a_{1Gj}T_G + a_{2Gj}T_G^2 + a_{3Gj}T_G^3$$

 $j = 18, 19, \dots, 27.$

Additional equations

To complete the definition of the reactor model, equations are needed for the pressure and the density of the solids stream within the reactor (gas density is calculated from the ideal gas law). The pressure drop in the gasifier is not very large and therefore the reactor pressure is expressed as a linear function of the coal bed height

$$P(z) = P(0) - z\Delta P,$$

where ΔP is the linear pressure drop coefficient in pressure per length and P(0) is the absolute pressure at the bottom of the reactor.

To calculate the local solids velocity and the void volume of the bed, both the bulk and raw densities of the solids are needed. The equation used to calculate the solids raw density is

$$\rho_{\text{raw}} = w_0 + w_1 W_c + w_2 W_w,$$

where $\rho_{\rm raw}$ is the raw density in weight per unit volume and the w are constants that are functions of the coal type. $W_{\rm c}$ is the weight fraction of the carbon in the solids and $W_{\rm w}$ is the weight fraction of moisture in the solids.

Two equations are used to calculate the bulk density. If the weight fraction of the carbon in the solids is greater than a specified value, then the equation used to calculate the solids bulk density is

$$\rho_{\text{bulk}} = w_3 - W_{\text{e}}.$$

Otherwise, we use

$$\rho_{\text{bulk}} = w_4 + w_5/(w_6 - W_c) + w_7 W_w + w_8 W_w^2$$

where ρ_{bulk} is the bulk density in weight per unit volume of reactor and the w are again constants that are functions of the coal type and the particle size distribution.

In the combustion zone, the bulk density is adjusted to compensate for ash prefluidization by using

$$\rho_{\text{bulk}} = \rho_{\text{bulk}} - w_{9}(1 - F_{\text{c}}/F_{\text{cb}}),$$

where w_9 is a constant, F_c is the molar flux of carbon in the solids in moles per minute per unit cross-sectional area of reactor, and F_{cb} is the molar flux of carbon entering the combustion zone.

Boundary conditions

The boundary conditions needed for the steady state simulation model are those that specify the input component molar fluxes and the temperatures of the solids and gas feed streams, and the inlet gas pressure. These conditions can be expressed as follows:

At the top of the reactor—

$$F_{jS} \qquad j = 1, 2, \cdots, 17$$

$$T_{S}$$

$$z = L;$$

At the bottom of the reactor—

$$F_{jG} j = 18, 19, \dots, 27$$

$$T_{G} P(0)$$

Solution procedure

The steady state equations given for the gasifier simulation model form a 29th-order two-point boundary value problem which must be solved iteratively to match the boundary conditions. The pressure equation is not coupled to the boundary value problem.

To begin the solution, the exit gas component molar fluxes and temperature are guessed, and using the known

Table 1 Reactor operating data.

	Ash reactor	Clinker reactor	Slagging reactor
Bed height (m; ft)	2.90; 9.50	2.90; 9.50	2.23; 7.30
Dry coal/oxygen (wt/wt)	2.80	2.64	2.50 (2.39)*
Steam/oxygen (mol/mol)	8.20	4.15	1.10 (1.12)*

Reactor internal diameter, 3.70 m (12.14 ft) Exit gas pressure, 2.84 MPa (28.0 atm)

Dry coal feed rate, 2067.7 kg/h-m² (423.5 lb/h-ft²)

Coal feed temperature, 78°C (172.4°F)

Table 2 Dry coal analysis; Roland seam subbituminous from Wyodak mine in Wyoming; wt %—dry basis (vs = volatile solids).

	Proximate	analysis		Ultimate a	inalysis
	carbon	43.3	16	С	66.753
Volat	ile matter	47.5	47.546 H ₂		5.266
Ash		9.13	38	N ₂	1.117
			S	0.735	
			Ash	9.138	
				O_2	16.991*
		Mode	el analysis		
N _o	0.6356	H ₂ O (vs)	7.3726	CH ₄ (vs)	12.8762
$\frac{N_2}{C}$	43.3160	$H_{2}^{2}(vs)$	0.0286	H _o S (vs)	0.5505
S	0.2171	CÓ _g (vs)	10.2350	$NH_3(vs)$	0.4860
Ash	9.1380	CO (vs)	5.2548	Tar (vs)	9.8896

^{*}By difference.

Table 3 Comparison of dry exit gas analysis obtained using calculated and actual results (Westfield; coarse Rosebud seam subbituminous coal from Big Sky mine in Montana).

	Main components of dry exit gas (mol %)				
	Calculated results for feed gas temp. of:		Westfie	eld data	
	385°C (725°F)	357°C* (675°F)	A	В	
H,	43.23	41.57	42.03	41.57	
H_{2} CO_{2}	31.05	31.83	31.08	31.61	
CO	15.81	15.47	15.44	15.44	
CH_4	9.91	11.13	11.45	11.38	

^{*}Methanation rate was increased by a factor of 10.

component molar fluxes and temperature for the inlet solids stream, the 29 differential equations are integrated from the top to the bottom of the reactor, using a variable-step fifth-order Runge-Kutta-Fehlberg method. If the calculated inlet gas component molar fluxes and temperature do not match the given boundary conditions, new exit gas values are estimated, and the calculations are repeated until the inlet gas boundary conditions are met within a reasonable tolerance.

The convergence scheme has been kept simple. The exit gas composition value guesses are adjusted by a simple gradient-like procedure, and the exit gas temperature is adjusted by a separate stochastic technique. A high-low averaging technique and a restart option are also used if convergence problems are encountered.

Simulation results

A computer program has been developed for the model presented in the previous sections and has been used to calculate temperature and composition profiles for three types of moving bed gasifiers. Most of the calculations have been made for a Lurgi-type reactor (ash discharge). For comparison, some calculations have been made for a clinker reactor (ash/clinker discharge) and for a slagging reactor (molten slag discharge).

Table 1 lists some of the operating data for the three reactors. The coal bed height used in the ash and clinker reactor calculations was 2.90 m (9.50 ft). Ordinarily, the clinker reactor bed height would be somewhat less than that of an ash reactor, about 2.77 m (9.10 ft) in this case, but the same height was used in the calculations to show the effect of equal bed height. The slagging reactor bed height was only 2.23 m (7.30 ft). A shorter bed height is needed for this reactor to maintain the combustion zone at the very bottom of the reactor; a burner is used to ensure that the slag discharge remains in a molten state. The combustion gas from the burner combines with the entering steam/oxygen stream to form the total feed stream to this reactor.

Table 2 gives the proximate, ultimate and simulation model analyses of the Roland seam subbituminous coal used in the calculations. The model analysis values in this table represent the dry coal feed composition for all of the computer runs and show how the volatile matter of the original coal was apportioned among the various volatile components.

To test the validity of the simulation results, two calculations were made to compare with data obtained in actual test runs of a Lurgi gasifier at Westfield, Scotland. Table 3 shows this comparison.

^{*}Burner gas included (mol %: O2, 9.24; N2, 69.32; H2O, 14.70; CO2, 6.74).

Although both coals are western subbituminous, some differences would be expected since the Westfield results are for Rosebud seam coal from Montana, and the computer simulation results are for Roland seam coal from Wyoming. The column A data for the Westfield results were taken from Table 5/11 in Woodall-Duckham [35] and the column B data were taken from Table 4 in that same report. The first column of the calculated results involves a carbon dioxide value matching that for the Westfield column A data. As can be seen, the carbon monoxide values also compare fairly well, but the calculated hydrogen is higher and the calculated methane is lower than the column A results. To adjust for this difference, the second column of the calculated results was made with an increased methanation rate (such that column 2 and column B hydrogen values matched). When this was done, the CO,, CO, and CH, values also compared very well. Thus, the simulation model can successfully match actual operating data.

• Temperature profiles

Figure 1 shows the calculated gas and solids temperature profiles for an ash reactor with a coal feed containing 34.67 wt % moisture. Distance is measured from the bottom of the reactor such that a z value of 1 represents the top of the gasifier where coal enters and raw gas is discharged. The distance from z = 1 to z = 0.67 is the drying zone for this run. In this zone, the gas and solids temperatures gradually increase as the coal dries. The distance from z = 0.67 to z = 0.29 is the devolatilization zone. In this zone, the gas and solids temperatures continue to rise gradually until near the end of the zone, where there is a very sharp rise in the solids temperature to a near temperature-pinch condition with the gas as the final pyrolysis products are released. The distance from z =0.29 to z = 0.15 is the gasification zone. In this zone, the gas temperature rises rapidly to its peak value, while the solids temperature continues its steady rise. The distance from z = 0.15 to z = 0.11 is the burning zone. In this zone the solids temperature rises rapidly to its peak value, while the gas temperature falls rapidly. The distance from z = 0.11 to z = 0 is the ash zone. Here the solids temperature drops rapidly to its exit value and the gas temperature continues to fall to its entering value, which is slightly lower than the solids discharge temperature. Thus, for this run, the drying zone used 33% of the reactor, the devolatilization zone used 38%, the gasification zone used 14%, the burning zone used 4%, and the ash zone used 11%.

Figure 2 shows the calculated gas and solids temperature profiles for a clinker reactor with a coal feed containing 34.67 wt % moisture. The temperature profiles are similar to the ones obtained for the ash reactor, except

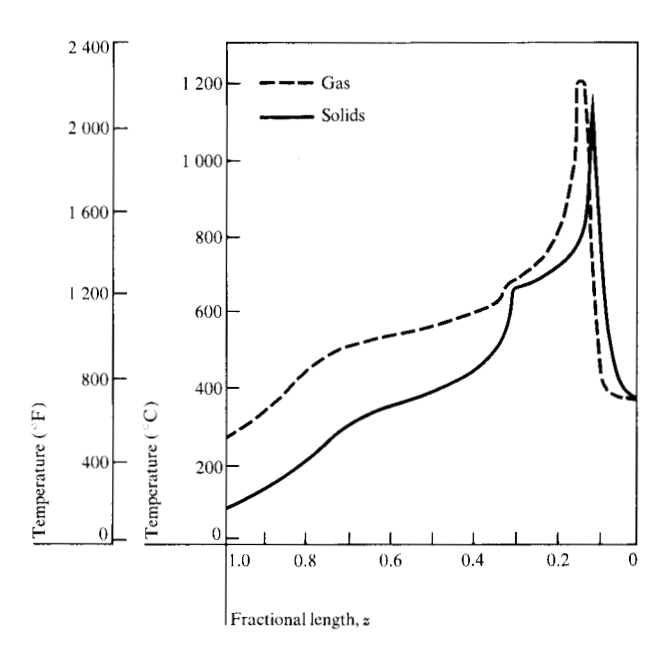


Figure 1 Temperature profiles for ash reactor; 34.67 wt % coal moisture. The fractional length z is measured from the bottom of the reactor; i.e., z = 1 represents the top of the gasifier and z = 0 the bottom of the gasifier.

Table 4 Effect of coal moisture on reactor operation.

	Weight percent moisture			
	34.67	27.00	20.40	12.40
Exit gas	10000			
temperature (°C; °F)	264; 506	305; 580	337; 638	372; 702
Zone length				
(fraction of				
total):				
drying	0.33	0.25	0.20	0.14
volatilization	0.38	0.41	0.43	0.46
gasification/				
burning	0.18	0.18	0.18	0.18
ash	0.11	0.16	0.19	0.22
Residence times				
(min):				
drying	19.2	15.7	12.9	9.7
volatilization	29.5	31.5	33.0	34.9
gasification/				
burning	31.1	31.3	31.2	31.2
ash	49.0	71.4	86.9	100.5
total	128.8	149.9	164.0	176.3

that the peak solids temperature is slightly higher and the peak gas temperature is much higher. The location of the gasification and combustion zones has also shifted somewhat towards the top of the gasifier. For this run, the

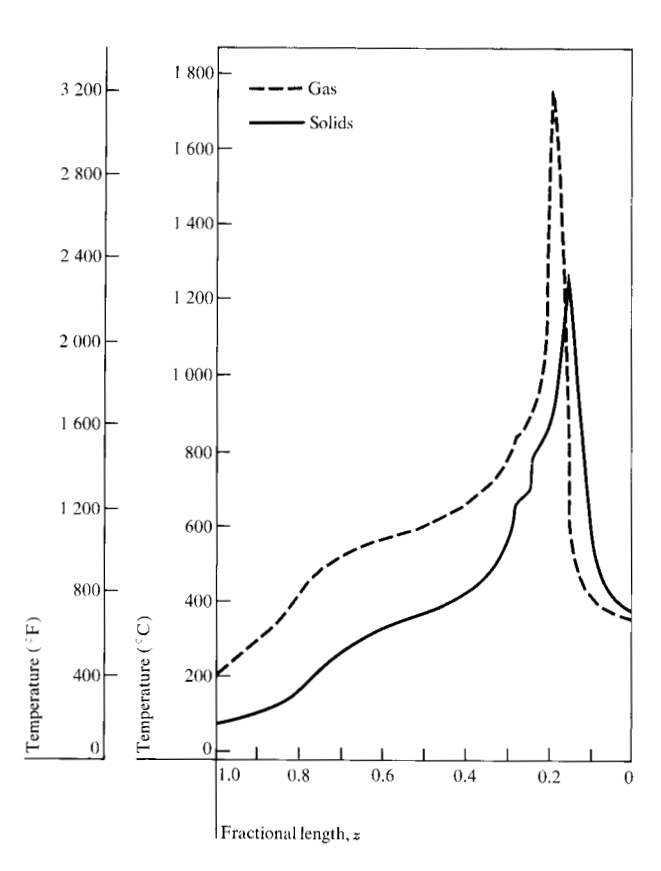


Figure 2 Temperature profiles for clinker reactor; 34.67 wt % coal moisture; z is defined in Fig. 1.

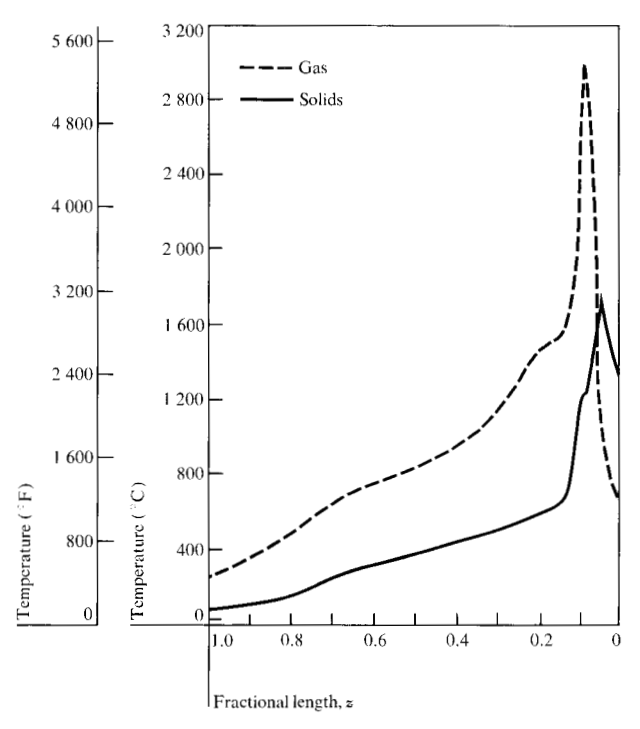


Figure 3 Temperature profiles for slagging reactor; 34.67 wt % coal moisture; z is defined in Fig. 1.

drying zone used 34% of the reactor, the devolatilization zone used 40%, the gasification zone used 8%, the burning zone used 3%, and the ash/clinker zone used 15%.

Figure 3 shows the calculated gas and solids temperature profiles for a slagging reactor with a coal feed containing 34.67 wt % moisture. Again, the temperature profiles are similar to the ash reactor profiles except that now the peak solids temperature is much higher and the peak gas temperature is very high. For this run, the drying zone used 44% of the reactor, the devolatilization zone used 43%, and the gasification, combustion, and slag zones used the remaining 13% of the reactor.

• Water-gas shift reaction

In some of the other gasifier modeling efforts, it was frequently assumed that the water-gas shift reaction is always at equilibrium in the gasification zone (e.g., see Yoon, Wei, and Denn [36]). To test this assumption, Fig. 4 shows a comparison of the calculated gas temperature and the water-gas shift equilibrium temperature for an ash reactor with a coal feed containing 12.40 wt % moisture. The water-gas shift equilibrium temperatures were obtained by using the calculated gas composition values to first find the equilibrium constant values. The temperatures corresponding to these values are plotted in Fig. 4. In this figure, the gasification zone lies between z = 0.40and z = 0.26. As can be seen, for z ranging from 0.40 to 0.37, the two temperature profiles are fairly close to each other. However, there is a severe discrepancy between the temperature profiles in the remainder of the gasification zone. Thus, in only about 21% of the gasification zone does it appear that one could reasonably assume that the water-gas shift reaction is in equilibrium. Also, the equilibrium temperature does not remain constant at its value leaving the gasification zone (z = 0.40), but it continues to rise gradually as the pyrolysis products and coal moisture are added to the gas stream in the devolatilization and drying zones. This creates a wide divergence in the gas and water-gas equilibrium temperatures in the exit gas stream, because the gas temperature drops rapidly as it nears the top of the reactor.

• Coal moisture

Table 4 shows the effect of changes in the feed coal moisture on the operation of an ash reactor. The first difference is the change in the exit gas temperature. As would be expected, the exit gas temperature increases when the moisture content of the feed coal is lowered. The principal difference, however, is the shift in the location of the reaction zones in the gasifier. Looking at the zone lengths, the drying zone goes from 33% down to 14% of the reactor length as the coal feed moisture is reduced from 34.67 to 12.40 wt %. At the same time, the

Table 5 Effect of inlet gas temperature on exit gas composition.

Component	Dry exit gas composition (mol %) for feed gas temperature (°C; °F) of:			
	329; 625	357; 675	385; 725	
H ₂	43.21	42.72	42.26	
N_2^2	0.66	0.67	0.67	
O_2^2	0.00	0.00	0.00	
CÔ,	31.56	30.89	30.36	
CO	13.49	14.56	15.46	
CH,	9.55	9.61	9.69	
H,S	0.18	0.18	0.18	
NH.	0.32	0.33	0.33	
tar	1.03	1.04	1.05	

devolatilization zone increases from 38% to 46% of the reactor. Since there is actually some overlapping of the devolatilization and drying zones, this increase would be expected to make up for the drop in drying zone length. The combined gasification/burning zone length is independent of coal moisture and it remains constant at 18% of the reactor length. The ash zone increases from 11% to 22%, reflecting the upward shift of the reaction zones as the coal moisture is reduced. The residence times in the various zones reflect a change similar to that found for the zone lengths. The total solids residence time increases from a little over 2 h to about 3 h as the moisture is decreased because of the increase in the length of the ash zone.

• Blast temperature

Table 5 shows how changes in the temperature of the steam/oxygen stream (blast temperature) affect the exit gas composition for an ash gasifier being fed coal with a moisture content of 34.67 wt %. The range of values for the inlet gas temperature is limited by two constraints. First, the inlet gas temperature must be high enough so that the exit gas temperature remains above the dew point temperature. Second, the inlet gas temperature cannot exceed the saturated steam feed temperature unless superheating is used. As can be seen, the H₂ and CO₂ content of the exit gas is reduced, and the CO and CH₄ content is increased, as the feed gas temperature is raised.

◆ Three reactor results

In this section, we will compare some of the calculated results obtained for ash (Lurgi), clinker, and slagging gasifiers. Table 6 gives the maximum gas and solids temperatures calculated for the three reactors. The main criterion for establishing whether a gasifier will discharge ash, ash/clinker, or molten slag is the steam-to-oxygen ratio in the feed gas. As shown in Table 6, the mole/mole steam-

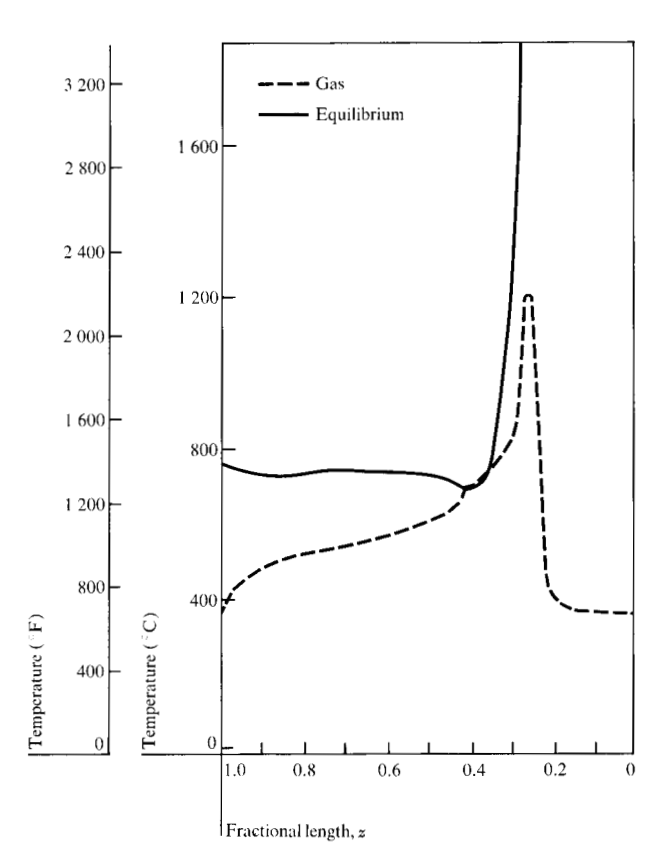


Figure 4 Equilibrium temperature profile for water-gas shift reaction and gas temperature profile; ash reactor; 12.40 wt % coal moisture; z is defined in Fig. 1.

Table 6 Calculated maximum reactor temperatures for the three reactors.

	Ash	Clinker	Slagging
Steam/oxygen (mol/mol)	8.20	4.15	1.10 (1.12)*
Solids temperature (°C; °F)	1175; 2147	1259; 2298	1731; 3148
Gas temperature (°C; °F)	1200; 2192	1756; 3192	2973; 5384

^{*}Burner gas included

to-oxygen ratio goes from a value of 8.20 to 4.15 to 1.10 for ash, ash/clinker, and slag discharges, respectively. Actually, in this case, because of the high reactivity of the Roland seam subbituminous coal used in the calculations, about 8% of the ash from the Lurgi gasifier is in the form of clinker. For the clinker reactor, about 56% of the ash is clinker. Because of the endothermic effect of melting ash, the maximum solids temperature in the

Table 7 Comparison of exit gas compositions (mol %-dry basis) for the three reactors.

Component	Ash	Clinker	Slagging*
Н.	42.72	35.63	18.53
N _a	0.67	0.80	1.07
$ H_{2} $ $ N_{2} $ $ O_{2} $ $ CO_{2} $	0.00	0.00	0.00
CÔ,	30.89	25.40	11.56
CO	14.56	25.19	51.79
CH,	9.61	11.23	14.86
H_2S^{\dagger}	0.18	0.21	0.26
NH,	0.33	0.37	0.46
tar	1.04	1.17	1.47

^{*}Burner gas removed.

Table 8 Comparison of reactor operation for the three reactors; coal moisture content of 34.67 wt %.

	Ash	Clinker	Slagging
Temperatures			
(°C; °F) for:			
exit gas	264; 506	204; 398	238; 461
feed gas	360; 680	359; 677	588; 1090
exit solids	366; 691	372; 702	1243; 2270
Residence times			
(min) for zones:			
drying	19.2	19.6	19.5
volatilization	29.5	30.5	26.3
gasification/			
burning	31.1	19.9	13.3
exit	49.0	68.7	15.8
total	128.8	138.7	74.9

clinker reactor is not much higher than that in the ash reactor. However, in the slagging reactor, the reactions in the gasification and burning zones are so violent that there is a substantial rise in the maximum solids temperature as compared to that in the ash reactor. Since the total amount of gas flowing in the reactor is reduced when the steam-to-oxygen ratio is lowered, it would be expected that the maximum gas temperature would rise substantially when going from an ash to a slagging reactor.

Table 7 gives a comparison of how the dry exit gas composition changes for the three different reactor types when they are fed the same amount of 34.67 wt % moisture content coal. As can be seen, the H₂ and CO₂ content of the exit gas is greatly reduced, and the CO and CH₄

content is greatly increased as we go from ash to clinker to slagging reactors. At the same time, the corresponding dry gas flow amount is reduced. Using the dry gas flow of the ash reactor as the base value, the clinker reactor dry gas flow is only 89% of that of the ash reactor, and the slagging reactor dry gas flow is only 70% of that of the ash reactor. It is interesting to note that the same type of behavior was obtained, only on a much smaller scale, when the inlet gas temperature was raised for the ash reactor (see Table 5).

Table 8 summarizes some of the calculated reactor operation parameters for the three gasifiers. The exit gas temperature for the clinker reactor is lower than that of the ash reactor because of the reduction in the amount of gas flow (the feed gas temperatures are the same for both reactors). The exit gas temperature for the slagging reactor is also lower than that of the ash reactor for the same reason, but it is not reduced as much because of the higher feed gas temperature for the slagger. As would be expected, the exit solids temperature for the slagging reactor is much higher than the solids discharge temperature for either the ash or the clinker reactor. Looking at the zone residence times, the drying time is essentially the same for all three reactors. The devolatilization time for the slagging reactor is a little less than that for the other two reactors. However, the gasification, burning and exit zone times are substantially less for the slagging reactor than for the ash and clinker reactors. The total residence time for the slagger is almost an hour less than that for the ash or the clinker reactor. This is partly due to the slagger bed height being shorter (see Table 1) and partly due to the much more severe operating conditions in the slagging reactor.

Summary

Mass and energy balances, along with kinetic, equilibrium, and thermodynamic equations, were used to derive a steady state plug flow simulation model for a moving bed gasifier. It has been shown that the results calculated by this model can successfully match actual operating data from a Lurgi gasifier at Westfield, Scotland for similar type subbituminous coals.

It was found that the water-gas shift reaction was in equilibrium only in a small section of the gasifier where the gas stream exits from the gasification zone. In the drying zone, devolatilization zone, and the remainder of the gasification zone, there is a wide divergence between the gas temperature and the temperature corresponding to the shift equilibrium.

Changes in the feed coal moisture for an ash reactor had an effect on both the exit gas temperature and the location of the reaction zones in the gasifier. As the feed coal moisture was reduced, the exit gas temperature increased and the location of the burning zone moved up the reactor. Thus, the ash zone increased from 11 to 22% of the reactor length as the coal moisure was reduced from 34.67 to 12.40 wt %.

Comparisons were also made among the calculated results for ash (Lurgi), clinker, and slagging gasifiers. Because of the endothermic effect of melting ash, the maximum solids temperature in the clinker reactor was not much higher than in the ash reactor, but there was a substantial rise in the maximum solids temperature in the slagging reactor. Since the total amount of the gas stream is lowered when going from an ash to a slagging reactor, there is a corresponding rise in the maximum gas temperature. The dry exit gas composition changes markedly for the three reactor types when they are fed the same amount of coal. In going from ash to clinker to slagging gasifier, the H, and CO, content of the exit gas is greatly reduced, and the CO and CH₄ content is greatly increased. Similar behavior for the exit gas was obtained only on a much smaller scale, when the inlet gas temperature was raised for the ash gasifier.

- **Nomenclature** char effective surface area ratio aconstants, $n = 1, \dots, 6$ a_n stoichiometric coefficient for component j in reac a_{ij} constants, $n = 0, \dots, 3$ a_{nGj} constants, $n = 0, \dots, 3$ a_{nSj} frequency factor for reaction i A_{i} A_n constants, n = 1, 16, 17 $A_{\rm GS}$ local gas-solids heat transfer area/volume ratio constants, $n = 1, \dots, 6$ b_{ni} constants, $n = 1, \dots, 4$ \boldsymbol{B}_n constants, n = 1, 16, 17constant $c_{\rm a}$ $c_{\mathbf{f}}$ constant constants, $n = 1, \dots, 4$ C_n constants, $n = 1, \dots, 4$ gas molar heat capacity C_{pG} solids molar heat capacity C_{pS} gas molar heat capacity for component j $\mathcal{C}_{\mathbf{pG}j}$ solids molar heat capacity for component j $C_{\mathbf{pS}j}$ $C_{\mathbf{c}}$ solids carbon concentration C_{G} total gas concentration C_{j}^{G} C_{n} C_{S} concentration of component j constants, n = 1, 16, 17total solids concentration
- constant constant D_{i} constant effective diffusion rate of oxygen through the ash D_{ea} effective diffusivity of component j for reaction i D_{ei} E_{i} activation energy for reaction i $F_{\rm e}$ molar flux of carbon in solids molar flux of carbon entering combustion zone molar flux of gas for component j molar flux of solids for component jlocal gas-solids heat transfer coefficient $h_{\rm GS}$ heat of reaction i ΔH_{i} constant H_{ci} reaction rate $k_{\rm e}$ film mass transfer coefficient k_i rate constant for reaction i overall rate constant for reaction (15) equilibrium constant for reaction i K_{i} M_{i} modified Thiele modulus for reaction i P absolute pressure ΔP linear pressure drop coefficient P(0)pressure at the bottom of the reactor reactor pressure at position z P(z)rate of reaction i $R_{\rm e}$ base drying rate gas constant R_z reaction rate solids particle radius average gas-solids absolute temperature absolute gas temperature absolute solids temperature local gas velocity u_{G} local solids velocity $u_{\rm s}$ constants, $n = 0, \dots, 9$ W_c weight fraction of carbon in solids weight fraction of moisture in solids $W_{\rm w}$ mole fraction of component j in solids X carbon fractional conversion coal critical moisture content X_{c} X_{w} mole fraction of moisture in solids mole fraction of component j in gas y_{j} z distance from reactor bottom constant α_{i} constant α' ratio of ash activity to commercial catalyst activity β_i reactor bed void fraction ε effectiveness factor for reaction i η_i CO-CO, distribution function for combustion products solids bulk density $ho_{
 m bulk}$ solids raw density $ho_{
 m raw}$ initial Thiele modulus gas energy flux ψ_{G}

solids energy flux

solids particle diameter

concentration of component j in gas

concentration of component j in solids

References

- M. McIntosh, "Mathematical Model of Drying in a Brown Coal Mill System 1. Formulation of Model," Fuel 55, No. 1, 47 (1976).
- M. McIntosh, "Mathematical Model of Drying in a Brown Coal Mill System 2. Testing of Model," Fuel 55, No. 1, 53 (1976).
- J. Campbell, "Pyrolysis of Subbituminous Coal in Relation to in-situ Coal Gasification," Fuel 57, No. 2, 217 (1978).
- J. Campbell, "Pyrolysis of Subbituminous Coal as it Relates to in situ Gasification Part 1: Gas Evolution," Report No. UCRL-52035, Lawrence Livermore Laboratory, Livermore, CA, March 1976.
- J. Campbell, "Pyrolysis of Subbituminous Coal as it Relates to in situ Gasification Part 2: Characterization of Liquid and Solid Products," Report No. UCRL-52035 Part 2, Lawrence Livermore Laboratory, Livermore, CA, June 1976.
- (a) S. Dutta, C. Wen, and R. Belt, "Reactivity of Coal and Char. 1. In Carbon Dioxide Atmosphere," *IEC Process Design Develop.* 16, No. 1, 20 (1977).
 (b) S. Dutta and C. Wen, "Reactivity of Coal and Char. 2. In Oxygen-Nitrogen Atmosphere," *IEC Process Design Develop.* 16, No. 1, 31 (1977).
- R. Taylor and D. Bowen, "Rate of Reaction of Steam and Carbon Dioxide with Chars Produced from Subbituminous Coals," Report No. UCRL-52002, Lawrence Livermore Laboratory, Livermore, CA, January 1976.
- M. Gibson and C. Euker, Jr., "Mathematical Modeling of Fluidized Bed Coal Gasification," Paper presented at the 68th Annual AIChE Meeting, Los Angeles, CA, November 1975.
- J. Fischer, J. Young, R. Lo, D. Bowyer, J. Johnson, and A. Jonke, "Gasification of Chars Produced under Simulated in situ Processing Conditions," *Annual Report No. ANL-76-131*, Argonne National Laboratory, Argonne, IL, December 1976.
- E. Hippo and P. Walker, Jr., "Reactivity of Heat-Treated Coals in Carbon Dioxide at 900°C," Fuel 54, No. 4, 245 (1975).
- E. Pyrcioch, H. Feldkirchner, C. Tsaros, J. Johnson, W. Bair, B. Lee, F. Schora, J. Huebler, and H. Linden, "Production of Pipeline Gas by Hydrogasification of Coal," Research Bulletin No. 39, Institute of Gas Technology, Chicago, IL, December 1972.
- A. Tomita, O. Mahajan, and P. Walker, Jr., "Reactivity of Heat-Treated Coals in Hydrogen," Fuel 56, No. 2, 137 (1977).
- 13. J. Moe, "Design of Water-Gas Shift Reactors," Chem. Engineering Progress 58, No. 3, 33 (1962).
- C. Wen, "Optimization of Coal Gasification Processes," R&D Report No. 66, Interim Report No. 1, Vols. 1 and 2, Office of Coal Research, Washington, DC, 1972.
- S. Vatcha, "Analysis and Design of Methanation Processes in the Production of Substitute Natural Gas," Ph.D. Thesis, California Institute of Technology, Pasadena, CA, March 1976
- A. Lee, "Methanation for Coal Gasification," Paper presented at the Symposium on Clean Fuels from Coal, Chicago, September 1973.
- M. Shah and R. Stillman, "Computer Control and Optimization of a Large Methanol Plant," J. Indus. Engineering Chem. 62, No. 12, 59 (1970).
- O. Levenspiel, Chemical Reaction Engineering, John Wiley & Sons, Inc., New York, 1972, p. 357.

- A. Kam, A. Hixson, and D. Perlmutter, "The Oxidation of Bituminous Coal—II. Experimental Kinetics and Interpretation," Chem. Eng. Sci. 31, No. 9, 821 (1976).
- R. Jenkins, S. Nandi and P. Walker, Jr., "Reactivity of Heat-Treated Coals in Air at 500°C," Fuel 52, No. 4, 288 (1973).
- 21. G. Sergeant and I. Smith, "Combustion Rate of Bituminous Coal Char in the Temperature Range 800 to 1700 K," *Fuel* 52, No. 1, 52 (1973).
- 22. I. Smith and R. Tyler, "Internal Burning of Pulverized Semi-Anthracite: The Relation Between Particle Structure and Reactivity," *Fuel* 51, No. 4, 312 (1972).
- I. Smith, "Kinetics of Combustion of Size-Graded Pulverized Fuels in the Temperature Range 1200-2270°K," Combust. Flame 17, No. 3, 303 (1971).
- I. Smith, "The Kinetics of Combustion of Pulverized Semi-Anthracite in the Temperature Range 1400-2200°K," Combust. Flame 17, No. 3, 421 (1971).
- M. Field, "Rate of Combustion of Size-Graded Fractions of Char from a Low-Rank Coal Between 1200°K and 2000°K," Combust. Flame 13, No. 3, 237 (1969).
- M. Field, "Measurements of the Effect of Rank on Combustion Rates of Pulverized Coal," Combust. Flame 14, No. 2, 237 (1970).
- 27. M. Nettleton, "Burning Rates of Devolatilized Coal Particles," *IEC Fundamentals* **6**, No. 1, 20 (1967).
- P. Weisz and R. Goodwin, "Combustion of Carbonaceous Deposits within Porous Catalyst Particles II. Intrinsic Burning Rate," J. Catalysis 6, 227 (1966).
- W. Lewis, E. Gilliland, and R. Paxton, "Low-Temperature Oxidation of Carbon," J. Indus. Engineering Chem. 46, No. 6, 1327 (1954).
- E. Gulbransen and K. Andrew, "Reactions of Artificial Graphite," J. Indus. Engineering Chem. 44, No. 5, 1034 (1952).
- 31. J. Kuchta, A. Kant, and G. Damon, "Combustion of Carbon in High Temperature, High Velocity Air Streams," *J. Indus. Engineering Chem.* 44, No. 7, 1559 (1952).
- 32. A. Parker and H. Hottel, "Combustion Rate of Carbon," J. Indus. Engineering Chem. 28, No. 11, 1334 (1936).
- 33. C. Tu, H. Davis, and H. Hottel, "Combustion Rate of Carbon," J. Indus. Engineering Chem. 26, No. 7, 749 (1934).
- 34. J. Arthur, "Reactions Between Carbon and Oxygen,"
- Chem. Soc. J., Faraday Trans. 47, 164 (1951).
 Woodall-Duckham Ltd., "Trials of American Coals in a Lurgi Gasifier at Westfield, Scotland," ERDA R&D Report No. FE-105, U.S. Department of Energy, Washington, DC, 1975.
- H. Yoon, J. Wei, and M. Denn, "A Model for Moving-Bed Coal Gasification Reactors," AIChE J. 24, No. 5, 885 (1978).

Received November 10, 1978; revised December 26, 1978

The author is located at the IBM Scientific Center, P.O. Box 10500, 1530 Page Mill Road, Palo Alto, California 94304.